

See discussions, stats, and author profiles for this publication at: <https://www.researchgate.net/publication/282644721>

# Cementitious Materials: Hydration Chemistry and Characterization

Research · October 2015

DOI: 10.13140/RG.2.1.1734.2163

---

CITATIONS

0

READS

468

1 author:



D. P. Bentz

National Institute of Standards and Technology

393 PUBLICATIONS 12,082 CITATIONS

SEE PROFILE

Some of the authors of this publication are also working on these related projects:



Increased use of fly ash in transportation infrastructure [View project](#)



Modelling with Cellular Automata [View project](#)

# CEMENTITIOUS MATERIALS: HYDRATION CHEMISTRY AND CHARACTERIZATION

D.P. Bentz

Building and Fire Research Laboratory  
100 Bureau Drive Stop 8621

National Institute of Standards and Technology  
Gaithersburg, MD 20899-8621 USA  
E-mail: dale.bentz@nist.gov

## Cement Production

Generally, cement clinker is produced by firing a mixture of clay and limestone in a kiln of some sort to a temperature of about 1450 °C [1]. At these high temperatures, the materials partially fuse and clinker nodules are produced. These nodules are then ground with a source of sulfate (gypsum, hemihydrate, or anhydrite) to produce Portland cement. The major four clinker phases are tricalcium silicate ( $C_3S$ ), dicalcium silicate ( $C_2S$ ), tricalcium aluminate ( $C_3A$ ), and tetracalcium aluminoferrite ( $C_4AF$ ) where in cement chemistry notation:  $C = CaO$ ,  $S = SiO_2$ ,  $A = Al_2O_3$ ,  $F = Fe_2O_3$ ,  $\bar{S} = SO_3$ , and  $H = H_2O$ . The clinker also contains many impurities, the three most important of which are the alkali (sodium and potassium) sulfates, free lime (C), and periclase ( $MgO$ ). The gypsum (or other sulfate) is added to regulate the setting of the cement, avoiding a very rapid setting due to hydration of the tricalcium aluminate phase. The clinker is ground in a ball or roller mill to produce a powder with a fineness on the order of  $400\text{ m}^2/\text{kg}$  and a median particle diameter on the order of  $10\text{--}15\text{ }\mu\text{m}$ . To produce cement paste, the cement powder is mixed with water, the mixture typically being characterized by the mass ratio of water to cement (the water-to-cement or w/c ratio).

## Clinker Phases

### *TRICALCIUM SILICATE*

Tricalcium silicate (alite) is the major component of most Portland cements, typically accounting for 50-70% of the overall clinker. It is fairly reactive and is largely responsible for the final properties of the cement paste, particularly up to 28 days of age. For example, its contribution to strength development is contrasted with those of the other cement phases in Fig. 1. When  $C_3S$  reacts with water, a mostly crystalline calcium hydroxide (CH) and a mostly amorphous calcium silicate hydrate ( $C-S-H$ ) gel are formed. The silicate ions have a low mobility in the cement paste pore solution and therefore the gel tends to deposit at the exterior of the hydrating cement grains. Thus, the gel is the “glue” that bonds the cement particles together, resulting in the dramatic transformation from a viscous suspension of cement particles in water into a rigid load-bearing “solid” material. Conversely, the calcium ions have a high mobility, so that CH crystals deposit wherever there is available pore space and larger crystals grow bigger at the expense of smaller ones via Ostwald ripening. The densities, molar volumes, and heats of formation of all of the clinker minerals are given in Table 1 [1].

Figure 1: Example strength development curves for the four major clinker phases of portland cement.

#### *DICALCIUM SILICATE*

Dicalcium silicate (belite) typically accounts for 15-30% of the clinker. It forms similar reaction products to the  $C_3S$ , but reacts at a significantly slower rate. Thus, it contributes to the longterm strength development (post 28 days) of cement-based materials as shown in Fig. 1. Because of its lower Ca/Si molar ratio, it produces significantly less CH than the tricalcium silicate, which can be of benefit when leaching of CH from the final structure is a concern.

#### *TRICALCIUM ALUMINATE*

Tricalcium aluminate accounts for 5-15% of the clinker. In the absence of a source of sulfate, it reacts very quickly with water to form calcium aluminate hydrates (such as  $C_3AH_6$ ). To avoid

Table 1: Physical Properties of Clinker Minerals and Silica Fume

| Mineral     | Density<br>(Mg/m <sup>3</sup> ) | Molar Volume<br>(cm <sup>3</sup> /mole) | Heat of formation<br>(kJ/mole) |
|-------------|---------------------------------|---|--------------------------------|
| $C_3S$      | 3.21                            | 71.                                     | -2927.8                        |
| $C_2S$      | 3.28                            | 52.                                     | -2311.6                        |
| $C_3A$      | 3.03                            | 89.1                                    | -3587.8                        |
| $C_4AF$     | 3.73                            | 128                                     | -5090.3                        |
| Gypsum      | 2.32                            | 74.2                                    | -2022.6                        |
| Silica fume | 2.22                            | 27                                      | -907.5                         |

this rapid reaction and the accompanying early stiffening of the cement paste, sulfate (gypsum) is added.  $C_3A$  reacts with sulfate and water to form ettringite ( $C_6A\bar{S}_3H_{32}$ ). Ettringite generally forms as long needles within the cement paste microstructure. When the sulfate is consumed, the ettringite becomes unstable (ettringite is also unstable at temperatures above 70 °C) and reacts with more of the aluminate to form the monosulfoaluminate phase ( $C_4A\bar{S}H_{12}$ ). The proportions of these different aluminate hydrates will thus depend on the sulfate content of the cement, and efforts are made at nearly all cement plants to determine the optimum sulfate content for a given clinker (usually based on maximizing 28-day compressive strength). Both the calcium and aluminate ions are relatively mobile (as are the sulfates), so ettringite tends to deposit wherever there is the most available pore space (such as in the interfacial transition zone (ITZ) cement paste regions between aggregates and bulk cement paste in conventional concrete). While  $C_3A$  reacts fairly quickly in a portland cement, its contribution to the overall strength of the final cement paste is fairly minor as illustrated in Fig. 1.

### **TETRACALCIUM ALUMINOFERRITE**

Tetracalcium aluminoferite typically accounts for 5-15% of the clinker. It is normally slowly reactive unless activated by special strength enhancers (such as triethanol amines), and therefore contributes only to longer term properties, and in a very minor way to overall strength as shown in Fig. 1. The iron generally has a low mobility within the pore solution and like the  $C-S-H$  gel deposits near its dissolution source.

### *Calcium Sulfates*

As mentioned previously, the calcium sulfate is added to control the setting characteristics of the cement pastes. When added in its hemihydrate ( $C\bar{S}H_{0.5}$ ) or anhydrite ( $C\bar{S}$ ) form (or if the dihydrate form dehydrates during the grinding process), the possibility for false setting exists. Here, the dehydrated gypsum quickly converts to the dihydrate ( $C\bar{S}H_2$ ) form and the newly formed crystals of gypsum interconnect, causing an early stiffening of the cement paste. Then, as the gypsum dissolves to participate in the cement reactions, the viscosity of the paste decreases once more (hence the term false setting). This is not to be confused with flash setting which typically occurs in an undersulfated cement paste due to the rapid conversion of  $C_3A$  to aluminate hydrates. In this case, the workability of the paste is permanently lost and cannot be recovered upon further mixing.

### **Potential Cement Composition from Bogue Calculation**

Generally, it is rather difficult to directly determine the composition of a given cement clinker or powder (although direct analysis via SEM/X-ray imaging of the cement clinker or the ground cement powder particles is a promising possibility [2, 3]). Instead, a potential composition is calculated from an oxide analysis of the cement, based on a procedure attributed to Bogue and outlined in Taylor [1]. The procedure assumes that the four major phases are present as  $C_3S$ ,  $C_2S$ ,  $C_3A$ , and  $C_4AF$ , that the  $Fe_2O_3$  occurs as  $C_4AF$ , and that the remaining  $Al_2O_3$  occurs as  $C_3A$ . Correcting the  $CaO$  content for the free lime (by subtraction), this leaves two equations (for  $CaO$  and  $SiO_2$ ) with two unknowns ( $C_3S$ , and  $C_2S$ ) which can be solved simultaneously. The final equations are then [1]:

$$C_3S = 4.0710 \times CaO - 7.6024 \times SiO_2 - 6.7187 \times Al_2O_3 - 1.4297 \times Fe_2O_3$$

$$C_2S = 2.8675 \times SiO_2 - 0.7544 \times C_3S$$

$$C_3A = 2.6504 \times Al_2O_3 - 1.6920 \times Fe_2O_3$$

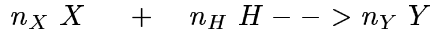
$$C_4AF = 3.0432 \times Fe_2O_3$$

where  $CaO$  is first corrected for the free lime content. Because this calculation ignores the  $MgO$  and alkali sulfates, the resultant phase mass fractions will not total 100%. The equations as written

apply only to cement clinker. When the oxide compositions are measured on a cement powder, the  $CaO$  needs to be further corrected for the calcium sulfate added to the cement powder to avoid flash setting.

### Hydration Reactions and Chemical Shrinkage

The basic chemical reaction for a cement mineral,  $X$ , forming hydration product  $Y$  can be written:



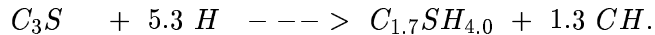
where  $n_X$ ,  $n_H$ , and  $n_Y$  represent the number of moles of  $X$ , water, and  $Y$  respectively. In cement-water systems, one peculiarity is that the hydration products occupy a smaller volume than the reactants, resulting in a net reduction in volume (chemical shrinkage) in a closed system. If  $V_X^M$  represents the molar volume of  $X$  in  $cm^3$ /mole, we can calculate the chemical shrinkage in  $cm^3/g$  of  $X$  as:

$$CS = \frac{n_Y * V_Y^M - (n_X * V_X^M + 18.0 * n_H)}{n_X * MW_X}$$

where 18.0 represents the molar volume of water and  $MW_X$  is the molecular mass of component  $X$  in g/mole ( $MW_X = V_X^M * \rho_X$  where  $\rho_X$  is the density of  $X$  in  $g/cm^3$  or  $Mg/m^3$ ). In a closed system, once the cement paste has achieved set, the chemical shrinkage will result in the creation of empty pores (self-desiccation) within the microstructure, and a reduction in the internal relative humidity of the sample (in turn inducing measurable autogenous shrinkage stresses and strains within the specimen).

### TRICALCIUM SILICATE

The generally accepted reaction for the hydration of  $C_3S$  is:



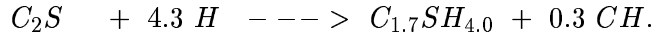
Whereas the molar volume and density of  $CH$  are well characterized, that of the  $C-S-H$  gel is much less so. Assumed values for the molar volumes, densities, and heats of formation of all the cement hydration products are given in Table 2 [4]. For chemical shrinkage, substituting the appropriate values into the above equation, we find  $CS = -0.0674 \ cm^3/g$  of  $C_3S$ .

Table 2: Physical Properties of Cement Hydration Products and Water

| Product               | Density<br>( $Mg/m^3$ ) | Molar Volume<br>( $cm^3$ /mole) | Heat of formation<br>(kJ/mole) |
|-----------------------|-------------------------|---------------------------------|--------------------------------|
| $CH$                  | 2.24                    | 33.                             | -986.1                         |
| $C_{1.7}SH_{4.0}$     | 2.12                    | 108.                            | -3283                          |
| $C_3AH_6$             | 2.52                    | 150.                            | -5548                          |
| $FH_3$                | 3.0                     | 69.8                            | -823.9                         |
| $C_6A\bar{S}_3H_{32}$ | 1.7                     | 735.                            | -17539.                        |
| $C_4A\bar{S}H_{12}$   | 1.99                    | 313.                            | -8778.                         |
| $H$                   | 1.0                     | 18.                             | -285.83                        |

## DICALCIUM SILICATE

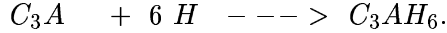
Very similar to the  $C_3S$ , the reaction for the hydration of  $C_2S$  is:



For chemical shrinkage, substituting the appropriate values into the above equation, we find  $CS = -0.0673 \text{ cm}^3/\text{g}$  of  $C_2S$ , nearly identical to that observed for the  $C_3S$  hydration on a per gram basis.

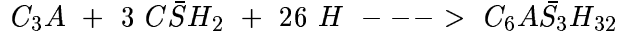
## TRICALCIUM ALUMINATE

As stated earlier, the  $C_3A$  can be involved in several different hydration reactions, depending on the sulfate present in the system. When sulfate is absent, a series of calcium aluminate hydrates will form, with  $C_3AH_6$  (hydrogarnet) being the ultimately stable form. Thus, we have:



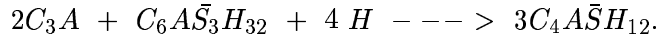
For chemical shrinkage, substituting the appropriate values into the above equation, we find  $CS = -0.174 \text{ cm}^3/\text{g}$  of  $C_3A$ . Thus, for this reaction, the chemical shrinkage is about three times that calculated for hydration of the silicates, on a per gram "cement" basis.

When sulfate is present, the conversion to ettringite takes place as:

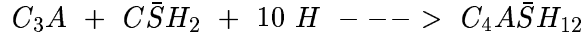


where a large quantity of water is consumed in the reaction. The calculated chemical shrinkage in this case is  $CS = -0.166 \text{ cm}^3/\text{g}$  of  $C_3A$  or  $-0.057 \text{ cm}^3/(\text{g of } C_3A \text{ and gypsum})$ .

Finally, when the ettringite becomes unstable (due to sulfate depletion), the ettringite converts to monosulfoaluminate via:



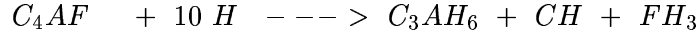
Here one calculates a chemical shrinkage of  $CS = -0.0856 \text{ cm}^3/\text{g}$  of  $C_3A$ , about one half of the value calculated for the previous 2 reactions. Alternately, adding the above two reactions together and dividing by three one obtains:



with an overall  $CS = -0.112 \text{ cm}^3/\text{g } C_3A$ .

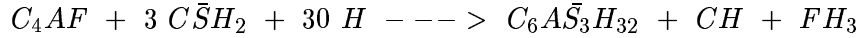
## TETRACALCIUM ALUMINOFERRITE

The reactions of tetracalcium aluminoferite are less well studied than those of the silicate phases and the  $C_3A$ . Reactions similar to those of  $C_3A$  occur with the iron possibly substituting into the ettringite and monosulfoaluminate phases or precipitating as an iron hydroxide ( $FH_3$ ) gel [1, 5]. Assuming the latter, one can write:



with a calculated chemical shrinkage of  $-0.116 \text{ cm}^3/\text{g } C_4AF$ .

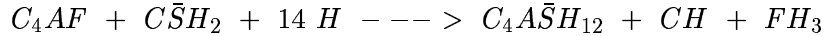
For the reaction with sulfate, one finds:



with a chemical shrinkage of  $-0.11 \text{ cm}^3/\text{g } C_4AF$ . Finally, for the conversion to monosulfoaluminate phase, one has:



with an accompanying chemical shrinkage of  $-0.065 \text{ cm}^3/\text{g}$   $C_4AF$ . Or, combining the above two reactions:



with an overall chemical shrinkage of  $-0.0802 \text{ cm}^3/\text{g}$   $C_4AF$ .

## Heat of Hydration

Based on the potential Bogue composition of a cement and the heats of hydration for the individual phases tabulated in Table 3, one can calculate the expected heat of hydration for a given cement. For practical purposes, using the experimentally measured heats of hydration for the pure phases provides a better fit to experimental data than those based on the heats of formation of the products and reactants. In general, in portland cement systems without mineral admixtures, there is a one-to-one correlation between heat of hydration and chemical shrinkage [4, 6, 7], as both are measures of the degree of hydration of the cement. The same cannot be said for strength, since there is always a certain amount of hydration which is necessary before any strength develops in the cement paste (this minimal hydration generally increases with an increase in w/c ratio). However, once a solid skeleton of unhydrated cement particles connected together by hydration products exists, strength is generally proportional to degree of hydration (as will be discussed in more detail later when the Power's gel-space ratio for strength prediction is introduced).

Table 3: Heats of Hydration of Clinker Minerals

| Mineral   | Measured heat of hydration (kJ/kg) | Calculated heat of hydration (kJ/kg) |
|-----------|------------------------------------|--------------------------------------|
| $C_3S$    | 517                                | 535                                  |
| $C_2S$    | 262                                | 224                                  |
| $C_3A^a$  | 1144                               | 1146                                 |
| $C_4AF^b$ | 725                                | endothermic?                         |

<sup>a</sup> Assuming production of monosulfoaluminate phase.

<sup>b</sup> From Fukuhara et al. [5].

## Hydration Kinetics

When a cement powder is first mixed with water, there is a small initial rapid release of heat (due to wetting and some initial dissolution of the cement), followed by a dormant or induction period during which very little hydration occurs. This can be seen in Figure 2 which plots the cumulative heat released vs. hydration time for two cements. For both cements, very little heat is released for the first 3-4 hours of hydration. Then, the reaction increases rapidly in an autoacceleratory manner, passes through a maximum rate and decays to a very slow rate which is maintained for days and even months. The exact causes of the induction period and how to regulate it are still unclear. Two main hypotheses are: 1) that it is due to the buildup of calcium ions in solution and ends when a critical supersaturation with respect to  $CH$  is reached and  $CH$  precipitation commences, or 2) it is due to the formation of a layer of relatively impermeable  $C-S-H$  gel on the surfaces of the cement particles which slowly dissolves away, allowing renewed contact between the water

and the cement particles, resulting in the more rapid hydration observed during the acceleratory period. Eventually, the reactions slow down due to spatial (space limiting) considerations, as the hydration products surrounding each cement particle begin to impinge and overlap, so that less and less of the cement particle surfaces are near to the capillary pore water.

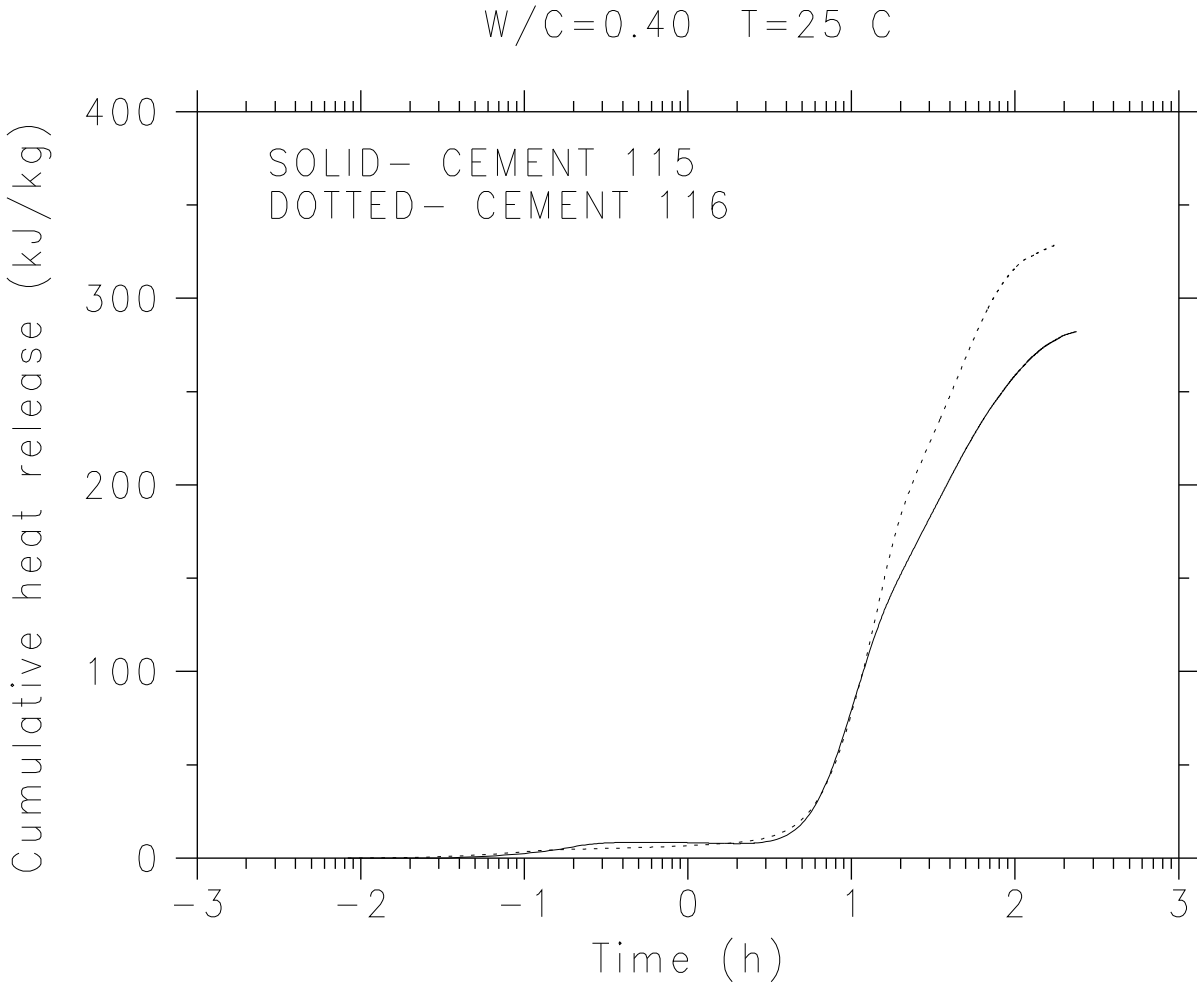


Figure 2: Experimental isothermal heat release curves for two cements [4].

To model these kinetics, Knudsen has introduced the “dispersion” models [8]. These models are based on particle size distribution considerations and have been shown to fit the hydration behavior and property evolution (heat release, chemical shrinkage, etc.) of a variety of cements [4, 8] at different w/c ratios and different temperatures. If we denote the degree of hydration of the cement (the fraction of the cement which has hydrated) by  $\alpha$ , the linear form of Knudsen’s dispersion model is:

$$\begin{aligned} \alpha &= 0 & t &< t_0 \\ \alpha &= \alpha_u * \frac{k(t-t_0)}{1+k(t-t_0)} & t &\geq t_0 \end{aligned}$$

where  $\alpha_u$  is the ultimate achievable degree of hydration,  $t_0$  is an induction time, and  $k$  is a rate constant. The parabolic dispersion model is similar in form but uses a square root of time behavior:

$$\alpha = \alpha_u * \frac{k\sqrt{(t-t_0)}}{1+k\sqrt{(t-t_0)}} \quad t \geq t_0.$$

Depending on the particular cement, one or the other of the two dispersion models will generally provide an excellent fit to the experimental data.

The early hydration kinetics (the first few days) can be followed by isothermal calorimetry as shown in Figure 2. Chemical shrinkage measurements can provide a measure of degree of hydration for longer times (up to 28 days and beyond), but only as long as the capillary porosity remains percolated so that the external water can be easily imbibed into the hydrating specimen [4, 9, 10]. Typically, the degree of hydration at longer times is assessed using loss on ignition measurements. A sample of the hydrated cement paste is ground to a powder, flushed with methanol, and heated in an oven at 105 °C. The mass after heating is recorded and the same specimen is then heated in a furnace at about 1000 °C for several hours. The final mass is recorded and the loss on ignition, *LOI*, is determined as:

$$LOI = \frac{m_{105} - m_{1000}}{m_{1000}}$$

where  $m_T$  indicates the mass of the specimen after heating to temperature  $T$  and a correction is normally made for the *LOI* of the unreacted cement powder itself. For many cements, at complete hydration, the *LOI* will be on the order of 0.23 g water/g cement powder [1]. Given the Bogue composition of the cement, the *LOI* at complete hydration can also be estimated using the coefficients provided in Table 4 [11].

Table 4: Non-evaporable Water Contents for Major Phases of Cement

| Cement Phase      | Coefficient<br>g water/g cement phase |
|-------------------|---------------------------------------|
| $C_3S$            | 0.24                                  |
| $C_2S$            | 0.21                                  |
| $C_3A$            | 0.40                                  |
| $C_4AF$           | 0.37                                  |
| Free lime ( $C$ ) | 0.33                                  |

### Influence of Temperature on Hydration Kinetics

As with most chemical reactions, those of cements are strongly influenced by temperature. The general approach to characterizing the variation of reaction rates with temperature is to use an Arrhenius analysis. In this case, the rate constant,  $k$  (such as those used in the Knudsen dispersion models provided above), varies with temperature according to:

$$k = k_0 e^{\frac{-E_a}{RT}}$$

where  $R$  is the ideal gas constant (8.314 J/(mole-K)),  $T$  is absolute temperature (K), and  $E_a$  is an activation energy. For many cements, observed activation energies are on the order of 40 kJ/mole [4]. In reality, each cement phase has its own activation energy and rate constants, but typically, they are analyzed in combination. Furthermore, the molar stoichiometry and molar volume of the  $C-S-H$  gel (and possibly other phases), and thus the chemical shrinkage, are a function of temperature [9].

## Silica Fume in High-Performance Concrete

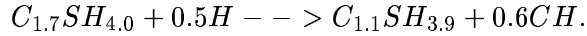
One of the “new” materials used in high-performance concrete (whose usage originated in the Nordic countries many years ago [12]), is silica fume. Silica fume is a byproduct from the production of silicon and silicon alloys. It is a microfine powder (average particle diameter less than  $1\text{ }\mu\text{m}$ ) that is typically 90-95% silica ( $\text{SiO}_2$ ) [1]. Its true specific gravity is 2.2 (Table 1), but it is very difficult to pack the light powder, so it is usually shipped as nodules or in slurry form. Its potential benefits in concrete are numerous. Because of its small size, it is able to efficiently fill in regions between cement particles, and between cement particles and aggregates (the ITZ region) [13]. Furthermore, it reacts with the calcium hydroxide and conventional  $\text{C-S-H}$  gel produced during cement hydration to produce a pozzolanic  $\text{C-S-H}$  gel (with a reduced Ca/Si molar ratio of 1.1). This gel, like that formed from the conventional hydration reactions, absorbs water, further reducing the capillary porosity of the cement paste matrix. The silica fume also acts as a slight accelerator of the hydration of the silicate phases in the cement powder.

For the reaction of silica fume with  $\text{CH}$  and conventional  $\text{C}_{1.7}\text{SH}_{4.0}$  gel, the following reactions are assumed in the NIST cement hydration model to be presented later in this lecture. For the direct reaction between silica fume and the calcium hydroxide formed during cement hydration the following is assumed:



with an assumed molar volume of  $101.8\text{ cm}^3/\text{mole}$  for the pozzolanic  $\text{C-S-H}$  gel [14]. In the NIST model, this reaction is assumed to occur at the silica fume particle surfaces when a diffusing  $\text{CH}$  species collides with a silica fume pixel [14].

When the silica fume is present in sufficient quantity (on the order of 5%), the conventional  $\text{C-S-H}$  gel formed during cement hydration will also be “converted” to the pozzolanic form via:



For the first reaction, one can calculate a chemical shrinkage of  $-0.20\text{ cm}^3/\text{g}$  silica fume, in general agreement with the experimental measurements of Jensen [15]. Thus, on a unit mass basis, silica fume contributes much more chemical shrinkage than the conventional clinker minerals. It also dramatically increases the “fineness” of the pore system. Taken together, these two properties of silica fume lead to a dramatic increase in self-desiccation and autogenous shrinkage in cement pastes containing silica fume. Regarding the reactivity of the silica fume, Lu et al. [16] have measured the degree of reaction of silica fume to be on the order of 45% for  $\text{w/c}=0.18$  cement pastes hydrated for 60 days, with silica fume contents ranging from 18-48%. The pozzolanic reaction is much more sensitive to temperature than conventional hydration, with an activation energy on the order of 83  $\text{kJ}/\text{mole}$  [14, 15].

## Characterization of Cement Powder

### Particle Size Distribution

The particle size distributions (PSD) of cements are typically assessed using x-ray sediograph or laser granulometry techniques [1]. It is a non-trivial measurement for cement powders due to their inherent tendency to flocculate into clusters of particles. Thus, the values measured often depend on the preparation technique (dispersion method, solvent, etc.). The PSD is typically reported as a cumulative curve of percent passing vs. particle diameter as shown in Figure 3. This figure provides results for one cement clinker ground to seven widely different finenesses [17]. To model the PSD of cements, data like that shown in Figure 3 is fit to a Rosin-Rammler distribution of the form:

$$\log n \log(100/R) = n * (\log n(x) - \log n(x_0))$$

where  $R$  is the mass percentage of material of particle size greater than  $x$  [1].  $x_0$  and  $n$  are constants characterizing the distribution,  $n$  being a measure of the breadth of the distribution and  $x_0$  indicating an “average” size (36.79% of the material is of size greater than  $x_0$ ).

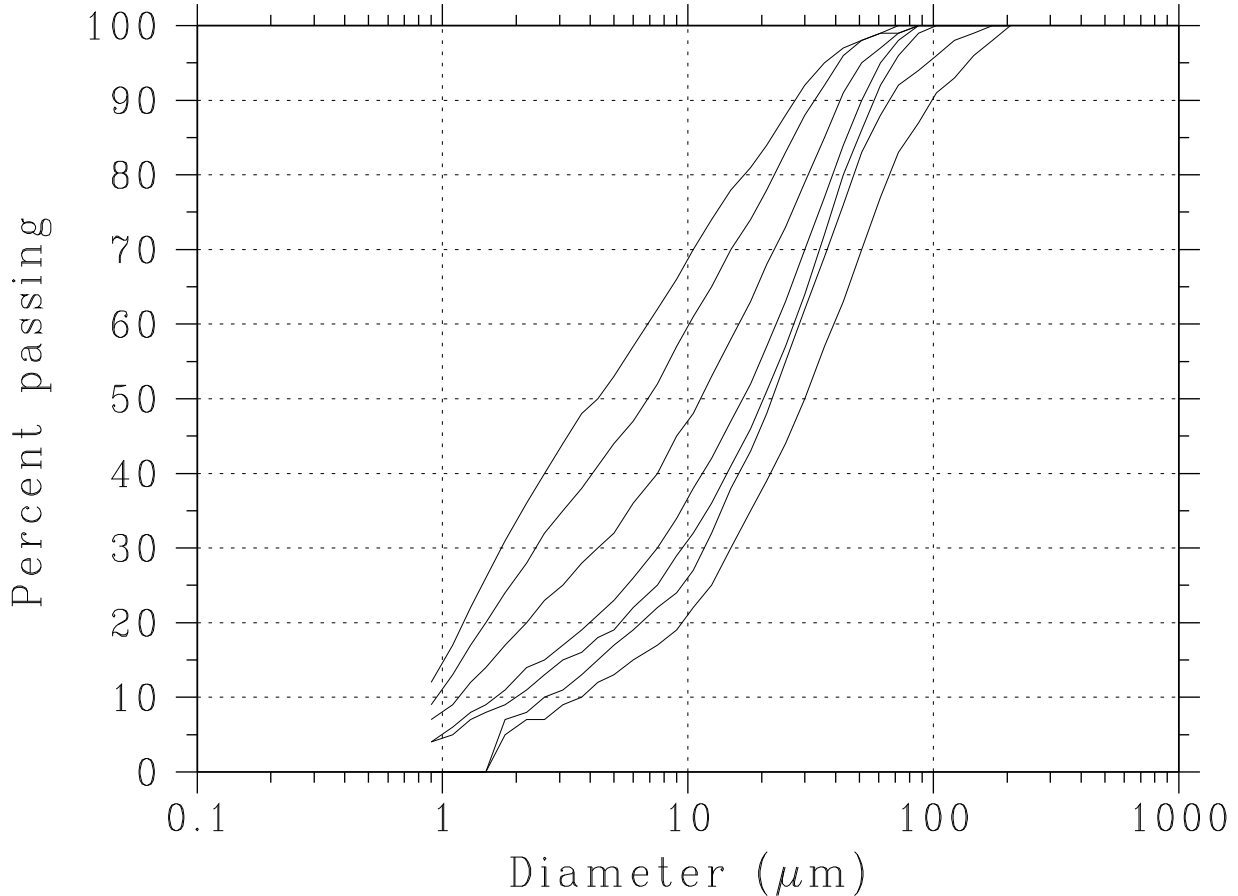


Figure 3: Measured particle size distributions for seven different portland cements from the same clinker [17]. From left to right, curves correspond to Rosin-Rammler average diameters,  $x_0$ , (and Blaine finenesses) of approximately 5  $\mu\text{m}$  ( $643 \text{ m}^2/\text{kg}$ ), 10  $\mu\text{m}$  ( $520 \text{ m}^2/\text{kg}$ ), 15  $\mu\text{m}$  ( $387 \text{ m}^2/\text{kg}$ ), 20  $\mu\text{m}$  ( $296 \text{ m}^2/\text{kg}$ ), 25  $\mu\text{m}$  ( $254 \text{ m}^2/\text{kg}$ ), 30  $\mu\text{m}$  ( $212 \text{ m}^2/\text{kg}$ ), and 40  $\mu\text{m}$  ( $163 \text{ m}^2/\text{kg}$ ).

The second common assessment of particle fineness is the Blaine fineness. This is based on the time required for a fixed volume of air to pass through a bed of packed cement powder [1]. The method is empirical in that it must be calibrated with cements of known fineness. The result is typically reported as a surface area in  $\text{m}^2/\text{kg}$  cement [1].

#### *Phase Composition and Distribution*

See the reprint “SEM/X-ray Imaging of Cement-Based Materials” [3] for information on this topic. While quantitative X-ray diffraction can provide information on the phase mass or volume fractions [1], only SEM imaging gives direct information on the distribution of the phases within individual cement particles.

## Cellular Automata Computer Modeling of Cement Hydration

### 3-D Reconstruction of Cement Particle Images

See the reprint “Three-Dimensional Computer Simulation of Portland Cement Hydration and Microstructure Development” [4].

### Cellular Automata Models of Cement Hydration

See once again the reprint “Three-Dimensional Computer Simulation of Portland Cement Hydration and Microstructure Development” [4].

## References

- [1] H.F.W. Taylor, Cement Chemistry, Thomas Telford, 1997.
- [2] P.E. Stutzman, Cement clinker characterization by scanning electron microscopy, *Cem Concr Aggregates* 13 (2) 109-114, 1991.
- [3] D.P. Bentz, P.E. Stutzman, C.J. Haecker, and S. Remond, SEM/X-ray imaging of cement-based materials, 7th Euroseminar on Microscopy Applied to Building Materials, Delft, The Netherlands, June 1999.
- [4] D.P. Bentz, Three-dimensional computer simulation of cement hydration and microstructure development, *J Am Ceram Soc* 80 (1) (1997) 3-21.
- [5] M. Fukuhara, S. Goto, K. Asaga, M. Daimon, and R. Kondo, Mechanisms and kinetics of  $C_4AF$  hydration with gypsum, *Cem Concr Res* 11 (1981) 407-414.
- [6] L.J. Parrott, M. Geiker, W.A. Gutteridge, and D. Killoh, Monitoring portland cement hydration: Comparison of methods, *Cem Concr Res* 20 (1990) 919-926.
- [7] T.C. Powers, Adsorption of water by portland cement paste during the hardening process, *Ind Eng Chem* 27 (1935) 790-794.
- [8] T. Knudsen, The dispersion model for hydration of portland cement I. general concepts, *Cem Concr Res* 14 (1984) 622-630.
- [9] M. Geiker, Studies of portland cement hydration: Measurement of chemical shrinkage and a systematic evaluation of hydration curves by means of the dispersion model, Ph. D. thesis, Technical University of Denmark, Copenhagen, Denmark, 1983.
- [10] D.P. Bentz, E.J. Garboczi, Percolation of phases in a three-dimensional cement paste microstructural model, *Cem Concr Res* 21 (1991) 325-344.
- [11] L. Molina, On predicting the influence of curing conditions on the degree of hydration, CBI Report 5:92 (Swedish Cement and Concrete Research Institute, Stockholm, 1992).
- [12] O.E. Gjorv, K.E. Loland, Condensed Silica Fume in Concrete, The Norwegian Institute of Technology, 1982.
- [13] D.P. Bentz, E.J. Garboczi, Simulation studies of the effects of mineral admixtures on the cement paste-aggregate interfacial zone, *ACI Mat J* 88 (5) (1991) 518-529.

- [14] D.P. Bentz, V. Waller, and F. deLarrard, Prediction of adiabatic temperature rise in conventional and high-performance concretes using a 3-D microstructural model, *Cem Concr Res* 28 (2) (1998) 285-297.
- [15] O.M. Jensen, The pozzolanic reaction of silica fume (in Danish), TR 229/90, Building Materials Laboratory, Technical University of Denmark, 1990.
- [16] P. Lu, G. Sun, J.F. Young, Phase composition of hydrated DSP cement pastes, *J Am Ceram Soc* 76 (1) (1993) 1003-1007.
- [17] D.P. Bentz, C.J. Haecker, An argument for using coarse cements in high performance concretes, *Cem Concr Res* 29 (1999) 615-618.
- [18] T.C. Powers, T.L. Brownyard, Studies of the physical properties of hardened portland cement paste, *J Am Concr Inst* 43 (1947) 101, 249, 469, 549, 669, 845, 993.